Vibrational relaxation of highly excited diatomics. I. Method, analysis, and application to HCl ($v \leq 7$)+CO_2 and N_2O

B. M. Berquist,[a] J. W. Bozzelli,[b] L. S. Dzelzkalns, L. G. Piper,[c] and F. Kaufman

Department of Chemistry, University of Pittsburgh, Pittsburgh, Pennsylvania 15260
(Received 19 August 1981; accepted 9 December 1981)

The infrared chemiluminescence method of Smith and co-workers is adapted to fast flow reactor conditions where a sensitive infrared detector views the vibrationally excited products of various generating reactions through a circularly variable filter in the absence or presence of added quencher molecules. The initial v-distributions are found to be totally unrelaxed vibrationally but thermalized rotationally. This allows the experimental measurement of vibrational relaxation rates of high v levels hitherto inaccessible. The modified Stern–Volmer method of analysis is described in detail. Its reference process is the rapid pumping rate constant $< 5 \times 10^3$ s^{-1} out of the field of view. $HCl^\dagger$ is generated by any one of four H atom reactions (with Cl_2, ICl, ClNO, or $SOCl_2$) or two Cl atom reactions (with HI or HBr), and its quenching rates by CO_2 or N_2O are measured. Quenching probabilities from about 5×10^{-3} to 0.5 per gas-kinetic collisions for $v = 1$ to 7 are found for both gases. The results are compared with the limited published data. Detailed discussion is deferred until the following paper which presents data for 18 additional quenchers.

I. INTRODUCTION

The properties of vibrationally highly excited polyatomic molecules have been studied successfully in many different ways, e.g., by thermal, chemical, or multiphoton laser activation methods. Such excited polyatomics seem to be well described, within certain limitations, by statistical theories and undergo rapid flow of internal energy. Collisional energy transfer processes of such species are characterized by very large rate constants and by weak dependence on the nature of the collision partner. Much less information is available on the behavior of highly excited diatomics whose vibrational level densities are necessarily very low and nearly constant as a function of energy. Quenching rate constants have been measured mainly for infrared-active hydrides and for CO by means of infrared chemiluminescence or laser induced fluorescence techniques. The former method normally uses exothermic atom–molecule reactions to prepare the system in an initial distribution of excited states, whereas the latter either uses single-quantum absorption, successive single-quantum absorption, or multiquantum absorption to prepare the v state(s) whose collisional relaxation is to be measured.

The largest effort so far has gone into HF(v) relaxation rate measurements and lesser efforts into DF, HCl, CO, and OH. The HF and HCl studies have concentrated mainly on the lower v's, i.e., $v = 1$ to 4 for two reasons: (1) the laser methods do not easily reach high v's; and (2) the chemiluminescence method, which is potentially capable of providing information for any excited state that is populated by the generating reaction, has been chiefly applied under conditions of extensive initial relaxation and severe depopulation of the highest attainable v states. The very substantial amount of work on exothermic atom–molecule reactions over the past 20 years has concerned itself mainly with the questions of energy disposal and detailed dynamics of the initial step, but much less so with subsequent collisional relaxation. Consequently, less progress has been made towards the experimental measurement and general understanding of collisional energy transfer of excited diatomics over wide ranges of v states and of collision partners.

The present paper is the first in a series devoted to $HCl^\dagger$ and $HF^\dagger$ relaxation studies. It presents the details of the experimental method, which is a close variant of the infrared chemiluminescence technique pioneered by Smith and co-workers.[1–3] The method differs from its forerunner principally in the time scale of the observation: the emission is monitored within $\lesssim 1$ ms of the formation of the excited states in 0.5 to 1.5 Torr He carrier gas. In the absence of efficient quenchers, the excited product species of the generating reaction are vibrationally unrelaxed but rotationally thermalized, because the initial concentrations of reactants (e.g., H and ICl) are as low as those in "arrested relaxation" experiments. In the modified Stern–Volmer analysis of the collisional cascade process, the reference process is the fast pumping rate constant, of order $\sim 5 \times 10^3$ s^{-1}, that removes the newly formed molecules from the field of view. Moderate spectral resolution is provided by a liquid nitrogen cooled circularly variable filter, and the signal is monitored by a selected, radiation limited InSb detector.

The results of this and the following paper are the first that describe the relaxation of HCl in $v = 4$ to 7. For unreactive quenchers where the collisional cascade process occurs by $\Delta v = 1$ steps there is surprisingly little information available: chemiluminescence studies of $v = 1$ to 3 by HCl, HBr, and CO_2[2]; and laser studies of $v = 1$ and 2 by HCl.[4–7] A recent paper from Polanyi's

[a] Present address: Westinghouse Bettis Atomic Power Laboratory, West Mifflin, PA 15122.
[b] Present address: Department of Chemistry and Chemical Engineering, New Jersey Institute of Technology, Newark, NJ 07102.
[c] Present address: Physical Sciences, Inc., Woburn, MA 01801.

 0021-9606/82/062972-12$02.10 © 1982 American Institute of Physics

Downloaded 14 Jul 2006 to 129.63.184.195. Redistribution subject to AIP license or copyright, see http://jcp.aip.org/jcp/copyright.jsp

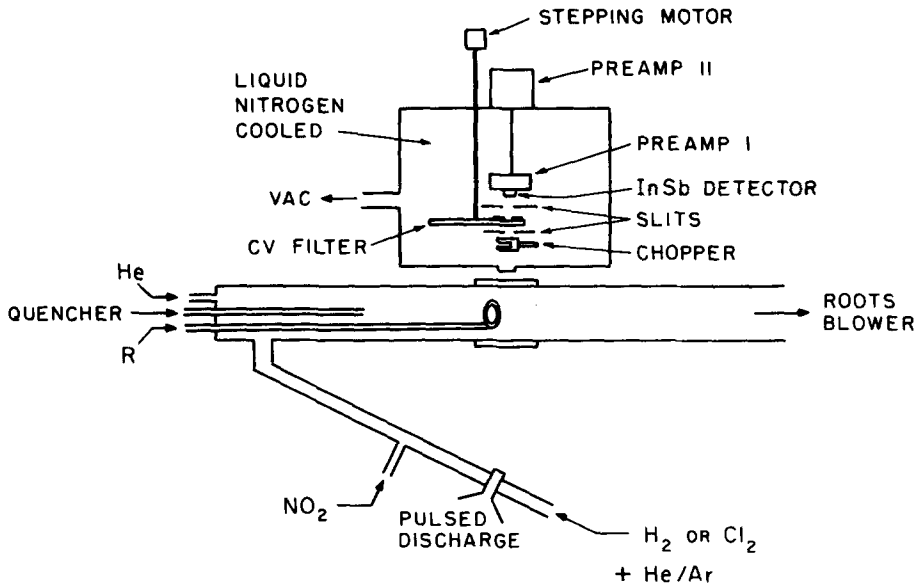

FIG. 1. Diagram of apparatus.

group[8] provides relative relaxation rate information for $v=2$ to 4 by CO_2 and includes the dependence of vibrational energy transfer efficiency on the rotational state of the $HCl^{\dagger}$ molecule. Fast-flow vibrational relaxation studies have been described by Liu *et al.*[9] for $CO^{\dagger}$ and by Kwok and Wilkins[10] for $HF^{\dagger}$ and $DF^{\dagger}$ with HF and D_2.

II. EXPERIMENTAL

A. The flow system

Figure 1 shows the flow reactor, a Pyrex tube of 5.3 cm i.d., 130 cm long, connected through a ball valve and 7.6 cm i.d. glass line to a high capacity Roots blower (Heraeus RA-2000, 550 $\ell\ s^{-1}$) backed by a large oil pump (Heraeus, E-225, 60 $\ell\ s^{-1}$). Maximum average flow velocities $\bar{u}$ of 1×10^4 cm s^{-1} (200 $\ell\ s^{-1}$) are obtained in the 0.5 to 1.0 Torr pressure range. The main He carrier gas flow (~150 cm^3 atm s^{-1}) enters the flow tube at its upstream end. Atomic reactant (H or Cl) is generated in a square wave modulated microwave discharge at a frequency of about 13 Hz in $He-H_2$ or $He-Cl_2$ mixtures containing about 0.4% H_2 or Cl_2 in a total flow of about 13 cm^3 atm s^{-1}. A small amount of Ar (~20%) is added to assure smooth operation of the discharge at the low frequency. A square-wave generator (Esterline Angus, Model F-1000) modulates the high voltage for the magnetron by about 400 V, from 1200 to 1600 V, by means of a power transistor (Delco DTS721) and a string of Zener diodes such that the discharge (Raytheon Microtherm, Evenson cavity) is maintained only at the higher voltage. The square-wave modulation frequency of the discharge is so low and the flow velocity so large that axial diffusion effects of precursor species such as H or Cl are negligible.

Both the molecular precursor (Cl_2, ICl, ClNO, HI, etc.) and the quencher gas are added through movable, fast-mixing injectors: The $HCl^{\dagger}$ precursor normally within the detector's field of view through a multiperforated glass loop, and the quencher (e.g., CO_2) through a movable, radially perforated glass or stainless steel tube, 10 to 50 cm farther upstream. Both additions are carried out with excess inert gas (He, Ar) to aid rapid mixing. The movable quencher addition tube helps distinguish problems associated with the upstream removal of atomic precursor species from true vibrational quenching effects. The important question of the speed of mixing of reactive $HCl^{\dagger}$ precursors was examined by adding NO through the glass loop to the main flow containing a small concentration of O atoms from an upstream O_2 discharge under flow conditions that closely approximated those of the $HCl^{\dagger}$ experiments. Judging by visual observation of the O + NO afterglow intensity, mixing was rapid and uniform, i.e., the onset of the glow at the loop was abrupt ($\lesssim$2 cm) in the axial direction and radially uniform to the flow tube wall. The question of axial mixing in the detector field of view will be further discussed below.

Small flows are measured by the pressure increase in a calibrated, evacuated volume using a pressure transducer (Validyne, model DP7, ±0.1 psi). The H_2 flow is measured using a capillary flowmeter, and the quencher flows are measured by the pressure increase method using larger (1 ℓ, 2 ℓ) volumes and a ±0.5 psi Validyne transducer. The large He-carrier flow is measured with a calibrated floating ball-type flowmeter (Fischer and Porter, No. 446-047). The chemiluminescence is viewed through a CaF_2 window. The field of view extends through a second CaF_2 window to a cold (77 K) background or to a heated blackbody source for calibration.

B. Infrared detection

Figure 1 also shows the evacuated, liquid nitrogen-cooled enclosure that houses the photovoltaic InSb detector (Barnes Engineering Co., 0.224 cm diameter selected for high resistance, 26 M Ω at 77 K) mounted on a copper disk heat sink attached to an aluminum inner housing that also holds the first stage of the preamplifier and the circularly variable filter (CVF). A tuning fork chopper (American Time Products, 227 Hz),

Downloaded 14 Jul 2006 to 129.63.184.195. Redistribution subject to AIP license or copyright, see http://jcp.aip.org/jcp/copyright.jsp

mounted directly in front of the CVF, is used for blackbody calibrations. The two-stage preamplifier was constructed following the work of Hall *et al.*[11] Its output signal is amplified using a phase-sensitive lock-in amplifier (Keithley, model 840) whose reference channel is connected to the pulse generator that controls the microwave discharge atom source. The output signal is displayed on a stripchart recorder.

The CVF (Optical Coating Laboratory, Inc.) consists of two 8.9 cm diameter, 180° segments mounted in a circular mount that cover the wavelength regions 1.2–2.4 and 2.25–4.5 μm, respectively. The filters have a nominal 1.5% to 2% bandpass, but since their spectral resolution must be known accurately for the purpose of interpreting the chemiluminescence signal in terms of vibrational populations, their bandpass was measured as a function of wavelength using a Beckman IR-11 spectrometer. It was found to be 2.15% for the shorter wavelength segment and from 2.1% to 1.7% for the other segment over the 2.6 to 4.4 μm range when a 3 mm wide entrance slit and a 2 mm exit slit was used with the CVF. Its peak transmission ranged from 50% to 60% for the first overtone emission of $HCl^\dagger$ and from 55% to 62% for the fundamental. The CVF is mounted on a stainless steel shaft that passes through a double-O-ring seal to a stepping motor on the outside of the vacuum enclosure. The motor rotates the CVF in one degree steps and is controlled by a pulse generator for automatic spectral scanning. The corresponding wavelength increments of 0.0067 and 0.0125 μm for the two CVF segments are about one quarter of the respective spectral bandpasses. With different gear arrangements, two or more degree steps could also be used. Most of the data were collected with one degree steps. Using the pulse generator and automatic scanning, the dwell time per step is variable from 0.1 to 1000 s. Most spectra were taken at 10 to 20 s per step. The stepping pulses could, of course, also be activated manually.

The CVF spectrometer-detector system was calibrated at regular intervals using a blackbody source (Barnes Engineering Co., model 11-120T). The noise-equivalent-power NEP of the InSb detector-filter combination was measured at 5.15 μm, using another CVF, at a blackbody temperature of 573 K, and found to be 3.6×10^{-14} W corresponding to 3.8×10^{6} photons per s when the transmission of the window, chopper, and CVF were taken into account. As is shown below, this high sensitivity is equivalent to the emission by a concentration of about 2×10^{8} cm^{-3} $HCl(v=7\rightarrow6)$ for $S/N=1$ and allows the measurement of $HCl^\dagger$ at sufficiently low precursor concentrations ($\sim5\times10^{-5}$ Torr) that unrelaxed, initial product distributions are determined with good accuracy.

C. Materials

He (HP grade, 99.995%), Ar (HP), H_2 (UHP, 99.999%), Cl_2 (HP, 99.5%), ClNO (HP, 97%), and ICl (Eastman Kodak, Inc. reagent) were used without further purification. Cylinder CO_2 gas (bone dry grade) gave erratic results indicating the presence of reactive impurities that remove H atoms. CO_2 was therefore prepared by repeated cooling and pumping of dry ice at 77 and 195 K.

D. Measurement of H atom concentration

It is important to know the absolute value of [H] in the main flow tube in order to assess its contribution to the collisional relaxation of $HCl^\dagger$ and also in order to know the rate of formation of $HCl^\dagger$ in the field of view. In its required concentration range of $(1-10)\times10^{12}$ cm^{-3}, it is difficult to measure by chemical titration, especially at the high flow velocities of the experiment. But since surface recombination of H is very slow, advantage may be taken of its much higher concentration in the side arm (Fig. 1) before the 30-fold dilution by the main flow of He. Measured additions of NO_2 through the titration inlet react with H quantitatively. For a typical main flow tube concentration of 2×10^{12} cm^{-3}, the concentration in the side arm is $\sim6\times10^{13}$ cm^{-3}, and the effective first-order rate constant for the $H+NO_2$ reaction in excess H is about 8000 s^{-1}, i.e., the reaction is virtually complete within a short distance. At the high flow velocity in the side arm, the much slower OH + OH reaction and the subsequent regeneration of one H for every three OH by $O+OH\rightarrow O_2+H$ may be neglected. The decrease of [H] is monitored by the $HCl^\dagger$ infrared chemiluminescence in the usual manner, i.e., ICl or Cl_2 is added at the CVF/IR detector. The extrapolation of the linear IR intensity vs added $[NO_2]$ plot to zero intensity gives the NO_2 flow equal to that of H, and division by total flow and multiplication by total concentration gives the desired H atom concentration in the main flow tube. A few check runs showed 20% to 50% fractional dissociation of H_2 in the discharge.

III. DATA ANALYSIS

A. Determination of vibrational state distributions

Figure 2 shows a typical chemiluminescent spectrum of the $H+ICl\rightarrow HCl^\dagger+I$ reaction under vibrationally unrelaxed conditions, i.e., without added quencher. The

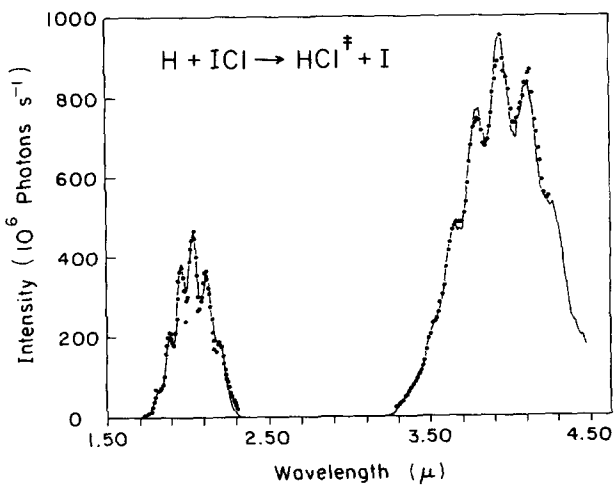

FIG. 2. Emission spectrum (fundamental and first overtone) of H + ICl without added quencher. Experimental points and computer fit (line).

Downloaded 14 Jul 2006 to 129.63.184.195. Redistribution subject to AIP license or copyright, see http://jcp.aip.org/jcp/copyright.jsp

unfolding of this low resolution spectrum of the fundamental and first overtone band progressions to yield vibrational level distributions follows earlier examples.[1-3] The emission intensity in a single rotational line $I_{v'j'\to v,j}$ (photons cm^{-3} s^{-1}), is given by

$$I_{v',j'\to v,j} = \frac{S_j F_j}{(2j'+1)}\left(\frac{\nu_{v'j'}}{\nu_{v'}}\right)^3 A_{v'v} N_{v'j'} = \frac{S_j F_j}{Q_R}\left(\frac{\nu_{v'j'}}{\nu_{v'}}\right)^3 \exp\left[\frac{B'j'(j'+1)}{kT}\right] A_{v'v} N_{v'} , \quad (1)$$

where S_j is the rotational line strength, F_j the Herman–Wallis factor (rotation–vibration interaction), $\nu_{v'j'}$ and $\nu_{v'}$ the rotational line and band origin frequencies, $A_{v'v}$ the Einstein band transition probability, Q_R the rotational partition function at 298 K, and $N_{v'j'}$ and $N_{v'}$ the concentrations of the $v'j'$ and v' (all j') $HCl^\dagger$ molecules. It is here assumed that the rotational states are collisionally thermalized at 298 K as is supported by experimental evidence described below.

The intensity from a unit population of emitters in level v' observed at wavelength λ taking account of the spectral resolution function (assumed triangular) of the CVF but omitting geometric and attenuation factors, is given by

$$U_{v'}(\lambda) = \frac{1}{N_{v'}}\sum_{j',j}\left[I_{v'j'\to vj}\left(1-\frac{|\lambda-\lambda_0|}{\alpha_\lambda \lambda}\right)\right] , \quad (2)$$

where λ is the CVF wavelength, λ_0 the wavelength of a particular rotational line in the interval $(\lambda-\alpha_\lambda)<\lambda<(\lambda+\alpha_\lambda)$, and α_λ the fractional FWHM resolution of the CVF in that wavelength range. The total emission from all the overlapping bands of the fundamental or first overtone region observed at wavelength λ is therefore

$$I^{(\lambda)}_{\Delta v=1 \text{ or } 2} = \sum_{v'v} f_{v'} U_{v'}(\lambda) , \quad (3)$$

where $f_{v'}$ is the fractional population in the v' state.

A computer program synthesizes the emission spectrum for a unit population of any desired band [Eq. (2)] in the fundamental or first overtone progression by calculating the transition frequencies using the Dunham potential of Rank *et al.*,[12,13] the Herman–Wallis factors calculated following Herman *et al.*,[14] the Einstein A values reported by Smith,[15] and the CVF resolution function, and summing over all rotational lines in each wavelength interval (0.001 μm). Figure 3 presents a synthetic spectrum for an assumed v' population distribution showing the contributions of each individual band as well as the total sum corresponding to Eq. (3).

The analysis of an experimental spectrum involves the inversion of Eq. (3), i.e., the calculation of a set of $f_{v'}$'s that optimizes the fit of the calculated $I(\lambda)$'s to the experimental intensities. This is accomplished in a computer program similar to CHIFIT by Bevington,[16] which minimizes

$$X^2 = \sum_{\lambda_n}[I(\lambda_n)^{\text{exp}} - I(\lambda_n)^{\text{calc}}]^2$$

as function of the $f_{v'}$'s by a nonlinear least squares method. Figure 2 gives an example of the calculated spectrum (line) along with experimental data (points)

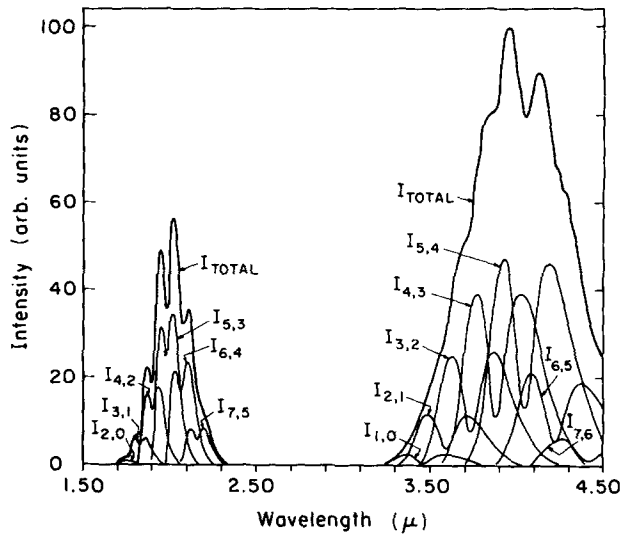

FIG. 3. Synthetic emission spectrum of $HCl^\dagger$ showing contributions of different v states to fundamental and first overtone. Assumed distribution: 0.15, 0.40, 0.70, 1.00, 1.20, 0.55, and 0.15 in $v=1$ to 7.

where the former corresponds to the relative populations (normalized to $v'=5$) given in the figure legend. This iterative program requires a reasonable initial guess of the $f_{v'}$'s, based either on visual inspection or on a preliminary fit that uses experimental intensities at a small number of selected wavelengths. Three to five iterations are normally sufficient for convergence, fewer if only four ($H+Cl_2$) rather than seven ($H+ICl$ or $ClNO$) v' levels are populated initially. The fact that both the fundamental and first overtone band intensities are monitored in most experiments provides an advantage in simultaneously fitting both progressions for a best fit. Substantially similar $f_{v'}$'s were obtained when only the fundamental, only the overtone, or both progressions were used in the analysis of $H+Cl_2$ emissions. However, the CVF cutoff at 4.5 μm makes the reliable analysis of $v'=6$ and 7 populations virtually impossible from the fundamental emission alone. It should be noted that the computer fits obtained with Smith's A values[15] were superior to those using the A values of Cashion and Polanyi[17] or of Herbelin and Emanuel.[18]

B. Determination of quenching rate constants

The modified Stern–Volmer analysis of the vibrational cascade process was used as first described by Hancock and Smith.[1] Its derivation need not be repeated here, but its principal assumptions and resulting expression will be presented. The assumptions include (1) steady-state, stirred flow reactor conditions with all source terms inside the field of view; (2) source terms for the vibrationally excited species are unaffected by the added quencher; and (3) cascade processes into and out of v levels include $\Delta v=1$ and 2 radiative terms but only $\Delta v=1$ collisional terms. The following working equation is obtained by summing the steady-state equations for a given v level and all levels above, both in the absence and presence of added quencher Q subtracting the two and dividing by $k_l N_v$:

Downloaded 14 Jul 2006 to 129.63.184.195. Redistribution subject to AIP license or copyright, see http://jcp.aip.org/jcp/copyright.jsp

$$\frac{N_v^0}{N_v} + \frac{A_{v+1,v-1}}{k_l}\left(\frac{N_{v+1}^0 - N_{v-1}}{N_v}\right) + \frac{k_p}{k_l}\sum_{m=1}^{m_{\max}}\left(\frac{N_{v+m}^0 - N_{v+m}}{N_v}\right) = 1 + \frac{k_{v,v-1}^Q}{k_l}[Q]\,. \tag{4}$$

Here, the N_v's are excited state concentrations, the superscript 0 indicates the absence of added quencher Q, $A_{v+1,v-1}$ is the Einstein coefficient for $\Delta v = 2$, k_p is the pseudo-first-order rate constant for the pumping loss, and

$$k_l \equiv k_p + \sum_{n=1}^{2} A_{v,v-n} + \sum_X k_{v,v-1}^X [X] \tag{5}$$

is the rate constant for loss out of the v level where X and k^X are concentrations and quenching rate constants of all other species, i.e., He, H_2, H, Cl_2, etc., and the A's are Einstein coefficients. Since k^{He} is very small, the other species are present in very low concentrations, and the A values are $\lesssim 100$, $k_l \simeq k_p$ to better than about 5%.

The pumping loss rate constant k_p is set equal to $\bar{u}/l$, where l is the distance from the injector to the downstream edge of the field of view, as further discussed below. The surface removal rate constant k_w is not included in k_l for reasons that are further described below. In experiments in which the injector was moved well upstream of the IR detector k_w was found to be about 300 s^{-1}, and information was obtained to suggest that surface collisions of $HCl^\dagger$ produced stepwise $\Delta v = 1$ relaxation.[19]

This fast-flow reactor mode differs from that of a true stirred-flow reactor as used by Smith and coworkers, and the application of Eq. (4) in our data analysis therefore requires further verification. Alternatively, other experimental modes may be used, such as movable source or movable quencher addition geometries in which reaction times are varied while the HCl species are monitored at the fixed IR detector. Although these methods work well in principle, their application here is difficult. If one attempts to drive the source reaction to completion, one must use large excess of HCl precursor. These gases may quench the high v levels of HCl and interfere with the analysis. For example, H and ClNO are very efficient quenchers of $HCl^\dagger$, ICl is moderately efficient, Cl_2 less so but also reacts less rapidly with H.

On the other hand, if one uses low precursor concentrations, the source terms are distributed along the flow tube. One then needs to model the entire reaction/relaxation system in order to extract a set of unknown quenching rate coefficients from a much larger set that includes notoriously irreproducible surface deactivation coefficients. This method also suffers from some of the uncertainties of fast-flow reactor analysis, e.g., the development of laminar flow, a complication which is well controlled in flowing afterglow ion molecule reaction kinetics[20] but which is aggravated here by the slow speed of the relaxation steps and by the less precise detector geometry.

This "brute force" method, in which the source (ClNO or ICl or Cl_2 injector) is moved along the flow tube, the coupled rate equations are integrated, and experimental $[HCl^\dagger]$ profiles are matched by computer modeling, was actually tried but later abandoned. It gave qualitatively consistent results for the higher v levels, but with excessive scatter and lack of reproducibility. When only a few v levels are populated, their kinetics may become sufficiently uncoupled, either by their initial concentration differences or by increasing the added quencher concentration that simple exponential decays are observed following an initial transient. Anlauf *et al.*[21] have measured HF ($v = 1$ and 2) relaxation by hydrocarbons in that manner, and Kwok and Cohen[22] and Kwok and Wilkins[10] have reported HF ($v = 1$, 2, and 3) relaxation rates by several polyatomics, but the choice and verification of the space-to-time conversion parameter constitutes a complex problem involving poorly characterized flow velocity distribution, radial diffusion and surface deactivation of excited species, distributed source terms, and discrimination by detector geometry.

Liu *et al.*[9] seem to have been the only ones to use the Stern–Volmer approach in a multilevel system $CO^\dagger + CO$ under fast-flow conditions. Their analysis assumes that k_p the volumetric pumping rate constant is much larger than the quenching rate constants $k_{v,v-1}^Q[Q]$, under their experimental conditions. This assumption is not justified, since the $k^Q[CO]$ terms are comparable in magnitude to k_p, i.e., of order 10^4 s^{-1}. The resulting difficulty cannot be rectified simply, because the term that is omitted involves $k_{v,v-1}^Q$, whereas the resulting equation [Eq. (10) in Ref. 9] is used to evaluate $k_{v+1,v}^Q$. Clearly, the two quenching steps, into and out of any given level, must both be considered. The correct Stern–Volmer-type equation that one obtains from steady-state analysis for a single v level is

$$\frac{N_v^0}{N_v} + \left(\frac{A_{v+1,v} + \sum_X k_{v+1,v}^X [X]}{k_l}\right)\left(\frac{N_{v+1} - N_{v+1}^0}{N_v}\right) = 1 + \frac{k_{v,v-1}^Q - k_{v+1,v}^Q \dfrac{N_{v+1}}{N_v}}{k_l}[Q] \tag{6}$$

if we neglect all $\Delta v = 2$ processes. It is this complication which prompted Hancock and Smith[1] to sum over all vibrational levels above v and thereby to replace the $k_{v+1,v}^Q$ term with the measured N_{v+m} and N_{v+m}^0 values. If Eq. (6) is to be used, one must start with the highest level where there is no N_{v+1} and where Eq. (6) reduces to the simple Stern–Volmer equation, and work downwards stepwise to lower v's.

In the present data analysis, the stirred-flow reactor mode is assumed to be applicable, and k_p is set equal to $\bar{u}/l$, where l is the axial distance from the injector to the downstream edge of the field of view. The full length of the field of view was determined experimentally by moving the injector in small increments (~0.5 cm) from well upstream (10–20 cm) to slightly downstream of the IR detector under constant conditions of the H + Cl_2 or H + ICl reaction without added quencher. A plot of IR signal at the spectral peak of the emission vs distance showed the expected break, i.e., a decrease in the I vs distance slope at the position where the injector was moved past the point where the emission filled the

Downloaded 14 Jul 2006 to 129.63.184.195. Redistribution subject to AIP license or copyright, see http://jcp.aip.org/jcp/copyright.jsp

TABLE I. Comparison of quenching rate constants with laser measurements.

	$HCl^{v=1}+CO_2$	$HCl^{v=1}+N_2O$	$HCl^{v=2}+HCl$	$HF^{v=5}+HF$
$k^Q(10^{-12}\ cm^3\ s^{-1})$	2.9[a]	1.4[a]	3.07[c]	151[f]
	2.9[b]		2.8[d]	
			2.6[e]	
This work	1.9	1.8	3.4	155

[a]Reference 4(a), 300 K, includes $V-V$ and $V-R,T$.
[b]Reference 4(b).
[c]Reference 7, 296 K.
[d]Reference 6.
[e]Reference 5, 296 K.
[f]Reference 23.

field of view. An average total length of 2.5 ± 0.3 cm was obtained from 24 experiments. In quenching experiments, the injector was usually placed 0.3 to 0.8 cm inside the field of view so that l was in the range 1.7 to 2.2 cm.

Although it is not possible to provide a direct proof that the stirred-flow approximation is valid, the following supporting evidence may be cited: If it is assumed that mixing is infinitely fast in the radial plane and that reaction and quenching occur under plug-flow conditions, both analytical solution and computer modeling show that the corresponding k_p is approximately $3\,\bar{u}/l$, and all k^Q would have to be multiplied by a factor of three. This analysis is presented in Appendix A. Comparison with published data clearly shows that such larger k^Q values would be far out of line. The rapid mixing of the gas streams at the injector and the mean diffusional displacement $(2Dt)^{1/2}$ of about 1 cm under typical experimental conditions at a mean free path of about 0.1 mm, lend qualitative support to the view that there is extensive mixing over an axial distance of about 1 cm.

In Table I, our k^Q values for various $HCl^\dagger$ and $HF^\dagger$ quenching processes are compared with other published studies that use direct laser excitation of single vibrational levels and follow the temporal decay of IR fluorescence. The agreement with the best available, direct data is seen to be quite good and does not suggest systematic deviations. Had the comparison of Table I shown a systematic trend, we would have used the laser results as external, absolute calibrations, but since the differences are fairly small and random, we make no corrections.

The principal value of the results presented in this and the following papers lies in the fact that although their absolute accuracy is not high, they cover many quenchers and a large range of v levels in a consistent, comparable manner. Clearly, the addition of small added quencher concentrations cannot perturb the mixing process in a major way, particularly since the carrier gas is mainly helium. One may thus argue the validity of a particular choice of k_p, but not the validity of the relative comparison for different v and Q. This simplified and somewhat arbitrary choice of k_p also prompted us to neglect the surface removal term k_w which is small compared with k_p and which may not be fully applicable in the mixing zone. The Einstein A coefficients which are even smaller were retained in the analysis, since they are clearly applicable.

Equation (4) is therefore simplified to the form

$$\frac{N_v^0}{N_v}+(k_p)\Big/\Big(k_p+\sum_{n=1}^{2}A_{v,v-n}\Big)\sum_{m=1}^{m_{\max}}\left(\frac{N_{v+m}^0-N_{v+m}}{N_v}\right)=1+\left\{(k_{v,v-1}^Q)\Big/\Big(k_p+\sum_{n=1}^{2}A_{v,v-n}\Big)\right\}[Q]\,. \tag{7}$$

Here, the second term on the left represents the cascade contribution; and when it dominates the first term, the accuracy of the analysis is reduced. This is aggravated when the particular v state is far below v_{max}, when its initial population is small compared with that of all the levels above it, and when the k^Q values increase strongly with increasing v, i.e., when there is a pile-up in the v state. For this reason, it is necessary to use two or three different generating reactions for each Q, i.e., $H+ICl$ for the high levels, $v=4$ to 7, $H+Cl_2$ for the intermediate levels, $v=2$ to 4, and $Cl+HBr$ for $v=1$.

IV. RESULTS AND DISCUSSION

A. Initial distributions

In this work, the emphasis is entirely on vibrational relaxation rather than on energy disposal. The analysis of the low resolution IR emission data presupposes that $HCl^\dagger$ is rotationally thermalized and that there are no hidden vibrational relaxation processes that compete with k_p and with $k^Q[Q]$. Extensive initial vibrational relaxation is therefore highly undesirable, since it implies that there are other quenching terms that make k_l considerably larger than k_p and that these terms are not identified under the experimental conditions. It was reassuring to find (a) that the initial vibrational distributions were indeed unrelaxed and (b) that there was no indication of sufficiently incomplete rotational relaxation to produce systematic deviations from the fit to theory as shown in Figs. 2 and 4 or to show small peaks arising from emission by high J states as reported by Sung and Setser.[24]

Six generating reactions were used in all, four of H, with Cl_2, NOCl, ICl, and $SOCl_2$ and two of Cl with HI and HBr. To measure the initial distributions, the atomic reactant concentration was kept low, of order 1 to 4×10^{12} cm^{-3}, and both the molecular reactant concentration and the pumping speed were varied. For each experimental condition, the spectrum was recorded and the relative vibrational populations obtained from the computer fit to the spectrum. The relative populations were plotted vs $[R]t$, where $[R]$ is the molecular reactant concentration, and t is the time of observation $l/\bar{u}\equiv k_p^{-1}$. The extrapolated populations as $[R]t\to0$ repre-

Downloaded 14 Jul 2006 to 129.63.184.195. Redistribution subject to AIP license or copyright, see http://jcp.aip.org/jcp/copyright.jsp

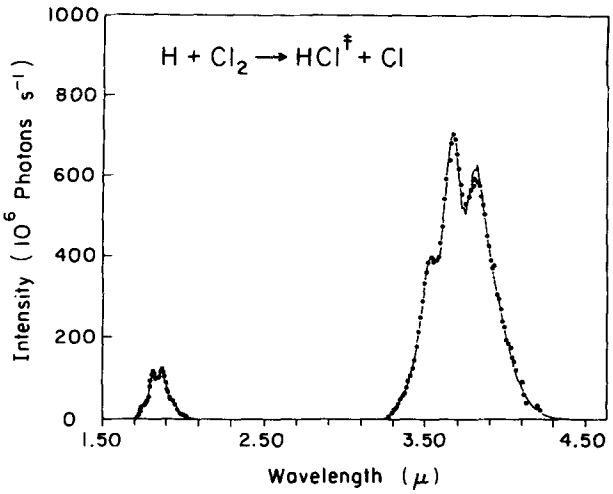

FIG. 4. Emission spectrum (fundamental and first overtone) of $H + Cl_2$ without added quencher. Experimental points and computer fit (line).

sent our best estimate of the initial distribution. In all cases, the plots were either totally flat or slightly rising for high v's and falling for low v's over the limited range of $[R]t$ examined. Figure 2 shows the computer fit for a typical H + ICl spectrum and Fig. 4 for an H + Cl_2 spectrum. Tables II–VI show the relative initial vibrational populations for the first five reactions in comparison to other published results, mainly from low pressure, arrested relaxation experiments. For the Cl + HBr reaction, we obtained population ratios for $v = 1$ and 2 of 1 : 0.12, in considerable disagreement with Maylotte *et al.*[33] who reported 1 : 0.4 in a single experiment, but in excellent agreement with the recent laser initiated measurement result of $1 : (0.11 \pm 0.05)$ by Zwier *et al.*[34] For the other five reactions, although there may be small discrepancies here and there (partly due to the choice of Einstein A coefficients), the agreement is quite good, and we may state that the vibrational distributions in the absence of added quencher are essentially unrelaxed, i.e., that the reference term in the Stern–Volmer expression does not contain residual quenching contributions that would make k_1 substantially larger than k_b.

TABLE II. Initial relative vibrational populations[a] of HCl from $H + Cl_2 \rightarrow HCl^{\dagger} + Cl$ normalized to $v = 2$.

$v=1$	2	3	4	5	Reference
0.32	1.0	0.77	>0.15	>0.05	25
0.28	1.0	0.92	0.1	•••	26
0.22	1.0	1.05	0.23	•••	27
0.26	1.0	1.07	0.095	•••	28
0.315	1.0	1.05	0.26	•••	29
0.33	1.0	0.98	0.22	0.01	This work

[a]Due to different choices of A values, the relative populations are not exactly comparable, but the corrections are small, ≤20% for the different v levels.

TABLE III. Initial relative vibrational populations[a] of HCl from $H + ClNO \rightarrow HCl^{\dagger} + NO$ normalized to $v = 4$.

$v=1$	2	3	4	5	6	7	Reference
•••	•••	0.85	1.0	1.04	0.50	0.10	30
0.39	0.70	1.09	1.0	•••	•••	•••	31
0.14	0.27	0.56	1.0	1.13	0.59	0.15	This work

[a]Due to different choices of A values, the relative populations are not exactly comparable, but the corrections are small, ≤20% for the different v levels.

TABLE IV. Initial relative vibrational populations[a] of HCl from $H + ICl \rightarrow HCl^{\dagger} + I$ normalized to $v = 4$.

$v=1$	2	3	4	5	6	7	Reference
0.37	0.77	0.98	1.0	1.18	1.25	0.93	30
0.45	0.55	0.75	1.0	1.0	0.85	0.40	29
0.46	0.58	0.88	1.0	1.09	0.84	0.37	This work

[a]Due to different choices of A values, the relative populations are not exactly comparable, but the corrections are small, ≤20% for the different v levels.

TABLE V. Initial relative vibrational populations[a] of HCl from $H + SOCl_2 \rightarrow HCl^{\dagger} + SOCl$ normalized to $v = 2$.

$v=1$	2	3	4	Reference
2.38	1.0	0.36	0.08	25
0.62	1.0	0.48	0.09	32
0.55	1.0	0.40	0.04	This work

[a]Due to different choices of A values, the relative populations are not exactly comparable, but the corrections are small, ≤20% for the different v levels.

TABLE VI. Initial relative vibrational populations[a] of HCl from $Cl + HI \rightarrow HCl^{\dagger} + I$ normalized to $v = 3$.

$v=1$	2	3	4	Reference
0.22	0.35	1.0	0.74	33
0.20	0.48	1.0	0.40	This work

[a]Due to different choices of A values, the relative populations are not exactly comparable, but the corrections are small, ≤20% for the different v levels.

B. Quenching of HCl^{v} by CO_2 and N_2O

Since the generation and analysis of experimental data is time consuming and must be repeated for each generating reaction, usually three reactions per quencher, and since it is the purpose of this study to provide a large matrix of data for many different quenchers, not as many repeat experiments could be performed for each subset as would normally be desirable. A representative sample of modified Stern–Volmer plots for CO_2 and N_2O are shown in Figs. 5 and 6, respectively. Figure 5(a) shows plots for HCl, $v = 4$ to 7, from H + ICl

Downloaded 14 Jul 2006 to 129.63.184.195. Redistribution subject to AIP license or copyright, see http://jcp.aip.org/jcp/copyright.jsp

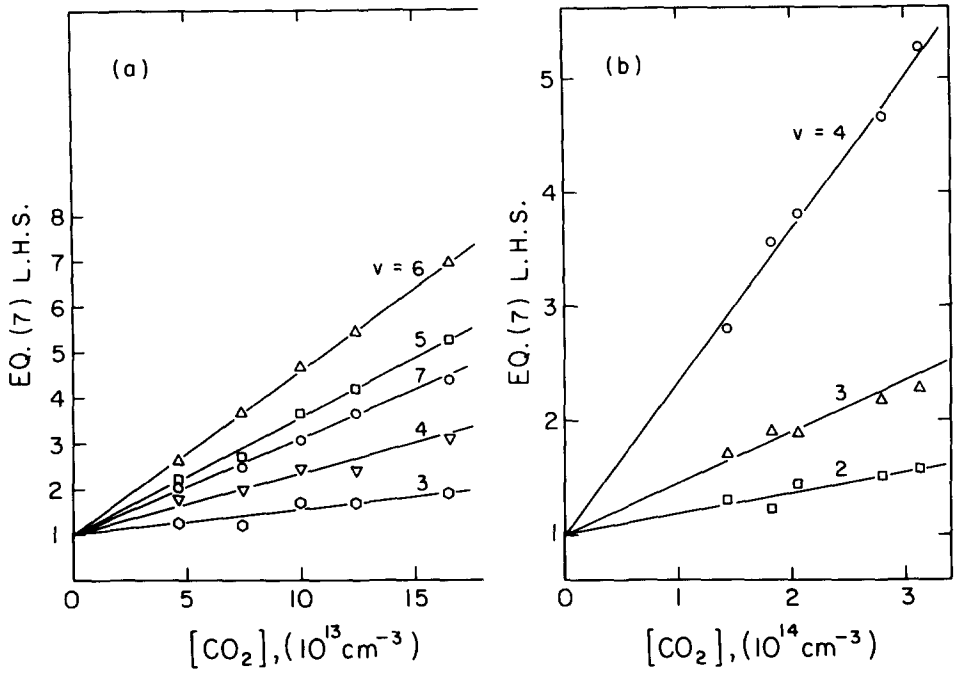

FIG. 5. Modified Stern–Volmer plot, Eq. (7), for $HCl^{\dagger} + CO_2$. (a) H + ICl generating reaction. (b) $H + Cl_2$ generating reaction.

and Fig. 5(b) for HCl, $v=2$ to 4, from $H + Cl_2$. Similarly, Fig. 6(a) shows the higher v states and Fig. 6(b) the lower v states in N_2O quenching experiments. In each plot, the ordinate, the left-hand side of Eq. (7), is plotted vs $[Q]$, and the slope is the desired k^Q divided by the reference rate constant which is usually very close to but slightly larger than k_b. Separate experiments were run for HCl, $v=1$, using the Cl + HBr reaction, since the extensive cascade and the sharply decreasing k^Q values with decreasing v would make its measurement in H + ICl or $H + Cl_2$ experiments unreliable. An error analysis in Appendix B shows that the accuracy of k^Q values is approximately $\gtrsim \pm 25\%$ to 30%.

Table VII shows experimental results for k^{CO_2} and Table VIII for k^{N_2O}. These are the first measurements for CO_2 in $v=5$ to 7 and for N_2O in $v=2$ to 7. For CO_2, $v=1$ to 3, the comparison with Ridley and Smith[2] shows good agreement for $v=1$ where the laser measurements[4(a),4(b)] (Table I) have reported higher values. For $v=2$ and 3, the agreement with Ridley and Smith[2] and with Bartoszek *et al.*[8] who normalized their relative k^{CO_2}'s to Ridley and Smith's $v=1$ value is moderately good, but our values are larger, as might be expected for the reasons given earlier, i.e., competing quenching steps in their slow-flow experiments. The discrepancy is somewhat larger for $v=4$ with Polanyi's group[8]

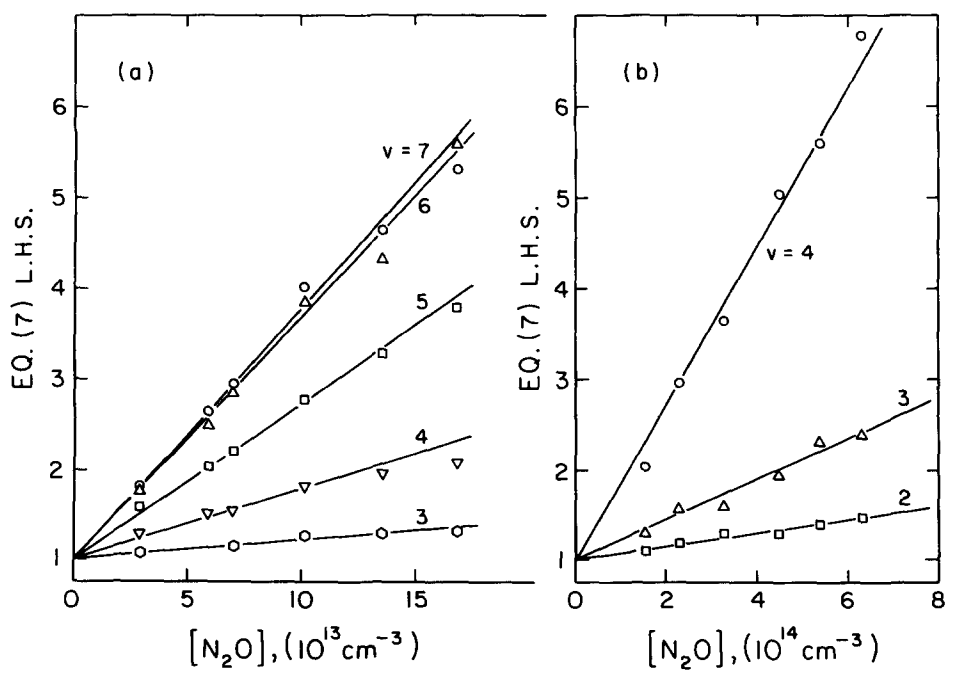

FIG. 6. Modified Stern–Volmer plot, Eq. (7), for $HCl^{\dagger} + N_2O$. (a) H + ICl generating reaction. (b) $H + Cl_2$ generating reaction.

Downloaded 14 Jul 2006 to 129.63.184.195. Redistribution subject to AIP license or copyright, see http://jcp.aip.org/jcp/copyright.jsp

TABLE VII. Quenching rate constants of $HCl^{\dagger}$ by CO_2, $T = 298$ K.

	$v=1$	2	3	4	5	6	7
$k(10^{-12}$ cm^3 s$^{-1})$[a]	1.9	9.0	23	70	139	173	102
P_{LJ}[b]	5.5×10^{-3}	2.6×10^{-2}	6.5×10^{-2}	0.19	0.38	0.47	0.40[c]
ΔE (cm^{-1}) for ν_3 of CO_2	537	433	330	227	124	22	−80
$k(10^{-12}$ cm^3 s$^{-1})$[e]	2.05	6.8	15.5				
[f]			14, 15[d]	31, 35[d]			
[g]	2.9						
[h]	2.9						

[a]Single standard deviation ~ 25%–30%.
[b]Based on Lennard-Jones collision frequency. Hard sphere P would be 1.48 times larger.
[c]P calculated for exothermic process.
[d]Based on $k_{1,0}$ from Ref. 2.
[e]Reference 2.
[f]Reference 8.
[g]Reference 4(a).
[h]Reference 4(b).

TABLE VIII. Quenching rate constants of $HCl^{\dagger}$ by N_2O, $T = 298$ K.

	$v=1$	2	3	4	5	6	7
$k(10^{-12}$ cm^3 s$^{-1})$[a]	1.8	4.5	12	45	96	149	152
P_{LJ}[b]	5.1×10^{-3}	1.3×10^{-2}	3.3×10^{-2}	0.12	0.26	0.40	0.40
ΔE (cm^{-1}) for ν_3 of N_2O	662	558	455	352	249	147	45
$k(10^{-12}$ cm^3 s$^{-1})$ Ref. 4(a)	1.4						

[a]Single standard deviation ~ 25%–30%.
[b]Probability based on Lennard-Jones collision frequency. Hard sphere P would be 1.55 times larger.

although the rate constant ratios $k_{4,3}^{CO_2}/k_{3,2}^{CO_2}$ are still in fair agreement, 3.0 vs 2.3.

The influence of the decreasing vibrational energy defect for $V-V$ transfer to ν_3 of CO_2 (2349 cm^{-1}) and N_2O (2224 cm^{-1}) is clearly shown for the higher v's. k^{CO_2} goes through a maximum at $v=6$ where there is near resonance ($\Delta\nu = 22$ cm^{-1}), whereas k^{N_2O} is comparable for $v=6$ and 7 ($\Delta\nu = 147$ and 45 cm^{-1}), even though it should rise monotonically to $v=7$. The often encountered $k^Q \propto v^n$ correlation is of limited use only for the lower levels, since k^Q becomes v independent or goes through a maximum farther up. We find n to be rising from 2.2 ($v=1$ to 3) to 3 ($v=3$ to 5) for CO_2 and from 1.3 ($v=1$ to 2) to 2.4 ($v=2$ to 3), 4.6 ($v=3$ to 4, probably in error due to too low a value for $k_{3,2}$), and decreasing to 3.4 ($v=4$ to 5) and 2.4 ($v=5$ to 6) for N_2O. To put these data on the basis of probability per collision P or its inverse Z the number of collisions required per vibrational energy transfer, the k^Q's were divided by k_{LJ}, the Lennard-Jones collision frequency, $\pi d_{AB}^2 (8RT/\pi M)^{1/2} \Omega_{AB}^{*(2,2)}$, where Ω values are from Ref. 35 using $d = 3.34$, 3.94, and 3.83 Å and $\epsilon/k = 345$, 195, and 232 K for HCl, CO_2, and N_2O,[36] and increasing $d_{HCl^{\dagger}} \propto B_v^{-1/2}$ for $v>0$ using spectroscopic values of the rotational constants B_v. The Lambert–Salter plots[37] of $\log(vZ)$ vs ΔE (cm^{-1}) neglecting rotational effects are shown in Fig. 7. They are reasonably linear for $\Delta E > 100$ cm^{-1}, their slopes are about 30% steeper than those of Fig. 4.20 in Ref. 37 and correspond to a value of C of about 6.4×10^{-3} cm in the equation $\ln(vZ) = C\Delta E$. (The slopes in Fig. 4.20 correspond to $C \simeq 4.9\times10^{-3}$ cm, not 5.3×10^{-3} as stated there.) The line is strongly displaced towards lower Z, i.e., larger probabilities of relaxation, from other infrared active quenchers. Thus, HCl ($v=6$) transfers a vibrational quantum at about half the Lennard-Jones and 70% of the hard sphere collision frequency, i.e., with an effective hard sphere cross section of about 30 Å^2. A comparison with the

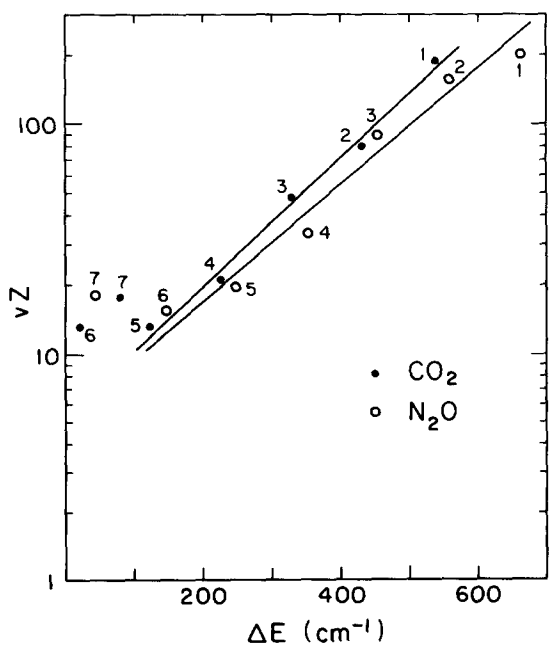

FIG. 7. Lambert–Salter plot for HCl + CO_2 and N_2O.

Downloaded 14 Jul 2006 to 129.63.184.195. Redistribution subject to AIP license or copyright, see http://jcp.aip.org/jcp/copyright.jsp

theory of Dillon and Stephenson[38] shows good agreement in magnitude for low v, but the theory predicts much too weak a v dependence, overestimating $k_{1,0}^{CO_2}$ by about a factor of 3 and underestimating $k_{4,3}^{CO_2}$ by a factor of 4. A more detailed discussion of the systematics of vibrational relaxation rates as function of v and Q is deferred until the following paper which presents results for a large number of quencher molecules.

ACKNOWLEDGMENTS

This work was supported by the Advanced Research Projects Agency and by the Air Force Office of Scientific Research under Grant No. AFOSR 80-0207A. L. G. P. appreciates stimulating and helpful discussion on spectral simulation and kinetic modeling with D. J. Bogan, Naval Research Laboratory, J. J. Sloan, National Research Council, Ottawa, and D. W. Setser, Kansas State University.

APPENDIX A: STERN-VOLMER ANALYSIS IN PLUG-FLOW APPROXIMATIONS

In this appendix, we calculate what values of k_l ($\sim k_p$) would have to be used if the plug flow approximation held accurately, i.e., if radial mixing were infinitely fast and axial mixing were negligible. Two calculations are summarized: (a) a computer model calculation for $HCl^{\dagger} + CO_2$, $v=1$ to 7, with H + ICl as generation reaction; and (b) an exact solution for the highest level $v=7$. The object in both cases is to examine possible inconsistencies between the stirred-flow and plug-flow analyses under conditions where the generating reaction is far from completed in the field of view of the detector.

Case (a). The differential equations for N_v^0 and N_v are

$$\bar{u}\frac{dN_v^0}{dz} = k_v[\mathrm{H}][\mathrm{ICl}] - (A_{v,v-1} + A_{v,v-2} + k_w)N_v^0 + A_{v+1,v}N_{v+1}^0 + A_{v+2,v}N_{v+2}^0 , \quad \text{(A1)}$$

$$\bar{u}\frac{dN_v}{dz} = k_v[\mathrm{H}][\mathrm{ICl}] - (A_{v,v-1} + A_{v,v-2} + k_w + k_{v,v-1}^{CO_2}[CO_2])N_v + (A_{v+1,v} + k_{v+1,v}^{CO_2}[CO_2])N_{v+1} + A_{v+2,v}N_{v+2} , \quad \text{(A2)}$$

$$\bar{u}\frac{d[\mathrm{H}]}{dz} = \bar{u}\frac{d[\mathrm{ICl}]}{dz} = -k_{tot}[\mathrm{H}][\mathrm{ICl}] , \quad \text{(A3)}$$

where z is the axial distance, all concentrations are functions of z, k_v is the rate constant of the H + ICl reaction into HCl^v, k_{tot} is the sum of all k_v, equal to 7.5×10^{-11} cm^3 s^{-1} (including HI + Cl branch),[29] the A's are the Einstein coefficients,[15] k_w is taken to be 300 s^{-1}, and the $k_{v,v-1}^{CO_2}$ values are taken from the results of the modified Stern–Volmer analysis. Typical experimental values of the other parameters are used: $\bar{u}=1.0\times10^4$ cm s^{-1}, $[\mathrm{H}]_0=2\times10^{12}$ cm^{-3}, $[\mathrm{ICl}]_0=4\times10^{12}$ cm^{-3}.

The sets of simultaneous equations are solved numerically using a fourth-order Runge–Kutta method and very small increments Δz. The observed emission is then calculated by summing $N_v^0(z)$ or $N_v(z)$ over the length l of the field of view and dividing by l, i.e., averaging the N_v's. These calculated values are then used in Eq. (7) and plotted in modified Stern–Volmer form as in Fig. 8. The plots are accurately linear for values of the ordinate up to ~3 and then curve slightly upward. But their most interesting property is that they require effective k_l values 2.9 to 3.5 times larger than $\bar{u}/l$ to give the originally assumed (stirred flow) values of $k_{v,v-1}^{CO_2}$.

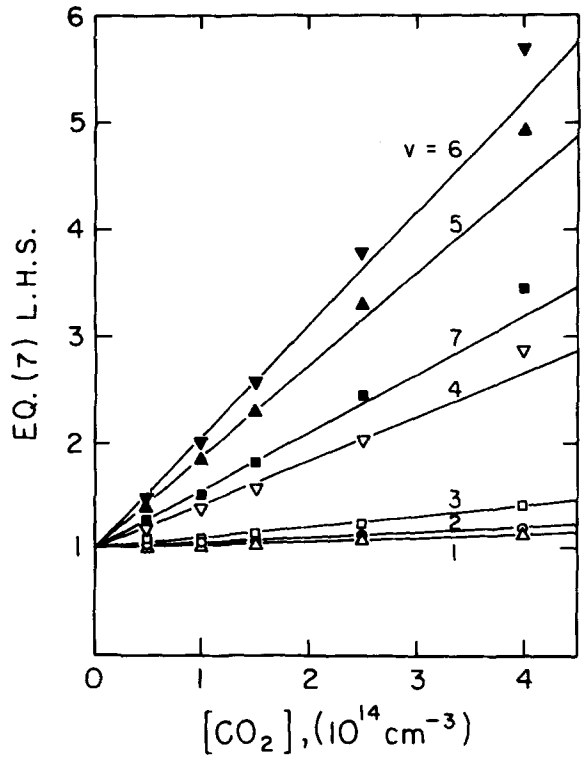

FIG. 8. Computer simulated Stern–Volmer analysis of assumed plug flow in field of view of IR detector.

Case (b). The above result is confirmed by an exact solution for the highest level $v=7$. Neglecting all A's and k_w, the equations are

$$\bar{u}\frac{dN_7^0}{dz} = k_7[\mathrm{H}][\mathrm{ICl}] , \quad \text{(A4)}$$

$$\bar{u}\frac{dN_7}{dz} = k_7[\mathrm{H}][\mathrm{ICl}] - k_{7,6}^{CO_2}[CO_2]N_7 , \quad \text{(A5)}$$

and the solutions are

$$N_7^0(z) = k_7[\mathrm{H}][\mathrm{ICl}](z/\bar{u}) ,$$

$$N_7(z) = \frac{k_7[\mathrm{H}][\mathrm{ICl}]}{k_{7,6}^{CO_2}[CO_2]}[1 - \exp(-k_{7,6}^{CO_2}[CO_2]z/\bar{u})] . \quad \text{(A6)}$$

Neglecting the consumption of H and ICl, setting $[\mathrm{H}][\mathrm{ICl}] \cong B$ and neglecting terms higher than z^2 in the expansion of the exponential,

$$N_7(z) = \frac{k_7 Bz}{\bar{u}}\left(1 - \frac{k_{7,6}^{CO_2}[CO_2]z}{2\bar{u}}\right) . \quad \text{(A7)}$$

Integrating $N_7^0(z)$ and $N_7(z)$ from $z=0$ to l and dividing by l yields

$$N_7^0 = \frac{k_7 Bl}{2\bar{u}} ; \quad N_7 = \frac{k_7 Bl}{2\bar{u}}\left(1 - \frac{k_{7,6}^{CO_2}[CO_2]l}{3\bar{u}}\right) . \quad \text{(A8)}$$

Dividing N_7^0 by N_7 and expanding $(1-y)^{-1} \approx 1+y$,

Downloaded 14 Jul 2006 to 129.63.184.195. Redistribution subject to AIP license or copyright, see http://jcp.aip.org/jcp/copyright.jsp

$$\frac{N_7^0}{N_7} = 1 + \frac{k_{7,6}^{CO_2}[CO_2]l}{3\bar{u}}, \tag{A9}$$

where comparison with the simple Stern–Volmer expression identifies $k_l \simeq 3\bar{u}/l$ rather than the originally assumed $\bar{u}/l$.

APPENDIX B: ERROR ANALYSIS

For the purpose of error analysis, Eq. (7) can be further simplified to

$$\frac{N_v^0}{N_v} + \sum_{m=1}^{m_{max}} \left(\frac{N_{v+m}^0 - N_{v+m}}{N_v}\right) - 1 = \frac{k_{v,v-1}^Q[Q]}{k_p}, \tag{B1}$$

which assumes that $\sum_{n=1}^{2} A_{v,v-n} \ll k_p$. Applying error propagation formulas,[39]

$$\frac{\sigma(k_{v,v-1}^Q)}{k_{v,v-1}^Q} = \left\{\frac{[\sigma(k_p/[Q])]^2}{(k_p/[Q])^2} + \frac{[\sigma(F)]^2}{F^2}\right\}^{1/2}, \tag{B2}$$

where the σ's are standard deviations, and F is the left-hand side of Eq. (B1). Since $k_p = \bar{u}/l = 0.886(\phi_T T)/(lr^2p)$, where ϕ_T ($cm^3\ s^{-1}$ at STP) is the total flow rate, T (K) the temperature, l (cm) the length of the field of view, r (cm) the tube radius, and p (Torr) the pressure, $[Q] = 9.65\times10^{18}\,\phi_Q p/\phi_T T$, where ϕ_Q ($cm^3\ s^{-1}$ at STP) is the quencher flow rate

$$k_p/[Q] \propto \frac{\phi_T^2 T^2}{\phi_Q l r^2 p^2}$$

and its fractional standard deviation is given by the error propagation expression

$$\frac{\sigma(k_p/[Q])}{k_p/[Q]} = \left\{4\left[\frac{\sigma(\phi_T)}{\phi_T}\right]^2 + 4\left[\frac{\sigma(T)}{T}\right]^2 + \left[\frac{\sigma(l)}{l}\right]^2 + 4\left[\frac{\sigma(r)}{r}\right]^2 + 4\left[\frac{\sigma(p)}{p}\right]^2 + \left[\frac{\sigma(\phi_Q)}{\phi_Q}\right]^2\right\}^{1/2}. \tag{B3}$$

The error in $k_p/[Q]$ is mainly due to the rather uncertain $\sigma(l)$ term and to $\sigma(p)$ in early experiments where p was measured by oil manometer to $\pm$(5% to 10%) accuracy. The more interesting and more variable $\sigma(F)/F$ term reduces to

$$\frac{\sigma(F)}{F} = \frac{[\sum_{m=0}^{max}(N_{v+m}^0 f_{N_{v+m}^0})^2 + \sum_{m=0}^{max}(N_{v+m} f_{N_{v+m}})^2 + f_{N_v}^2(\sum_{m=0}^{max} N_{v+m}^{0^2} + \sum_{m=0}^{max} N_{v+m}^2)]^{1/2}}{\sum_{m=0}^{max} N_{v+m}^0 - \sum_{m=0}^{max} N_{v+m}}, \tag{B4}$$

where $f_N \equiv \sigma_N/N$ is the fractional precision with which a given vibrational population is determined from the spectrum. If it is further assumed that f is constant for all N_v's, the numerator of the right-hand side of (B4) is simplified to

$$\sqrt{2}\, f\left[\sum_{m=0}^{max}(N_{v+m}^0)^2 + \sum_{m=0}^{max}(N_{v+m})^2\right]^{1/2}.$$

The important feature of (B4) is the decreasing magnitude of its denominator as m_{max} is increased, i.e., as the particular v level is farther down the vibrational ladder. If there is a pile up in a lower level, because its quenching rate constant is smaller than those for higher v's, this will redistribute the N_v's without greatly affecting their sum, i.e., the denominator will approach zero, and the errors in F and in k^Q will grow unacceptably large. Trial calculations for a typical case where the k_v^Q's increase in the sequence 1 : 0.9 : 1.1 : 5 : 11 : 17 for $v = 2$ to 7 (corresponding to Q = HCl, see following paper) show that when enough quencher is added to reduce $N_{v=7}$ by a factor of three, $k_{7,6}$, $k_{6,5}$, and $k_{5,4}$ can be determined to good accuracy (2 to $3f$), but $k_{4,3}$ and below cannot ($\gtrsim 12f$), because below $k_{5,4}$ the rate constants are much smaller. This can be alleviated either by adding more quencher or by using a different generating reaction, such as $H + Cl_2$, that produces HCl in $v \leq 4$. The magnitude of f_N was found to be in the range 0.1–0.15 as deduced from the reproducibility of spectrum inversion ($\lesssim 0.1$) and from overall reproducibility of k^Q determination. Quenching rate constants are thus seen to be accurate to $\pm$25%–30%.

[1]G. Hancock and I. W. M. Smith, Appl. Opt. **10**, 1827 (1971); G. Hancock, C. Morley, and I. W. M. Smith, Chem. Phys. Lett. **12**, 193 (1971); G. Hancock, B. A. Ridley, and I. W. M. Smith, J. Chem. Soc. Faraday Trans. 2 **68**, 2117 (1972).

[2]B. A. Ridley and I. W. M. Smith, J. Chem. Soc. Faraday Trans. 2 **68**, 1231 (1972).

[3]J. R. Airey and I. W. M. Smith, J. Chem. Phys. **57**, 1669 (1972).

[4](a) L. Doyenette, F. A. Adel, A. Chacroun, M. Margottin-Maclou, and L. Henry, J. Chem. Phys. **63**, 1479 (1975); (b) H. L. Chen, J. C. Stephenson, and C. B. Moore, Chem. Phys. Lett. **2**, 593 (1968).

[5]B. M. Hopkins and H-L. Chen, J. Chem. Phys. **57**, 3816 (1972).

[6]I. Burak, Y. Noter, A. M. Ronn, and A. Szöke, Chem. Phys. Lett. **17**, 345 (1972).

[7]S. R. Leone and C. B. Moore, Chem. Phys. Lett. **19**, 340 (1973).

[8]F. E. Bartoszek, R. D. H. Brown, and J. C. Polanyi, J. Chem. Soc. Faraday Trans. 2 **75**, 434 (1979).

[9]Y. S. Liu, R. A. McFarlane, and G. J. Wolga, J. Chem. Phys. **63**, 228, 235 (1975).

[10]M. A. Kwok and R. L. Wilkins, J. Chem. Phys. **63**, 2453 (1975).

[11]D. N. B. Hall, R. S. Aikens, R. Joyce, and T. W. McCurrin, Appl. Phys. **14**, 450 (1975).

[12]D. H. Rank, D. P. Eastman, B. S. Rao, and T. A. Wiggins, J. Opt. Soc. Am. **52**, 1 (1962).

[13]D. H. Rank, B. S. Rao, and T. A. Wiggins, J. Mol. Spectrosc. **17**, 122 (1965).

[14]R. Herman, R. Rothery, and R. J. Rubin, J. Mol. Spectrosc. **2**, 369 (1958).

[15]F. G. Smith, J. Quant. Spectrosc. Radiat. Transfer **13**, 717 (1973).

[16]P. R. Bevington, *Data Reduction and Error Analysis for the Physical Sciences* (McGraw-Hill, New York, 1969), p. 222.

[17]J. K. Cashion and J. C. Polanyi, Proc. R. Soc. London Ser. A **258**, 529 (1960).

[18]J. M. Herbelin and G. Emanuel, J. Chem. Phys. **60**, 689 (1974).

[19]B. M. Berquist and F. Kaufman (unpublished results).

[20]E. E. Ferguson, F. C. Fehsenfeld, and A. L. Schmeltekopf, Adv. Atom. Mol. Phys. **5**, 1 (1969).

[21]K. G. Anlauf, P. H. Dawson, and J. A. Herman, J. Chem.

Downloaded 14 Jul 2006 to 129.63.184.195. Redistribution subject to AIP license or copyright, see http://jcp.aip.org/jcp/copyright.jsp

Phys. **58**, 5354 (1973).
[22]M. A. Kwok and N. Cohen, J. Chem. Phys. **61**, 5221 (1974).
[23]G. M. Jursich and F. F. Crim, J. Chem. Phys. **74**, 4455 (1981).
[24]J. P. Sung and D. W. Setser, J. Chem. Phys. **69**, 3868 (1978).
[25]R. L. Johnson, M. J. Perona, and D. W. Setser, J. Chem. Phys. **52**, 6372 (1970).
[26]K. G. Anlauf, D. S. Horne, R. G. MacDonald, J. C. Polanyi, and K. B. Woodall, J. Chem. Phys. **56**, 1561 (1972).
[27]F. Menard-Bourcin, J. Manard, and L. Henry, J. Chem. Phys. **63**, 1479 (1975).
[28]K. Tagamake and D. W. Setser, J. Phys. Chem. **83**, 1000 (1979).
[29]J. P. Sung, R. J. Malins, and D. W. Setser, J. Phys. Chem. **83**, 1007 (1979).
[30]M. A. Nazar, J. C. Polanyi, and W. J. Skrlac, Chem. Phys. Lett. **29**, 473 (1974); J. C. Polanyi and W. J. Skrlac, Chem. Phys. **23**, 167 (1977).
[31]F. Menard-Bourcin, J. Menard, and L. Henry, C. R. Acad. Sci. (Paris) **274**, 1134 (1972).
[32]W. Bardoff and H. Heydtmann, Ber. Bunsenges. Phys. Chem. **82**, 649 (1978).
[33]D. H. Maylotte, J. C. Polanyi, and K. B. Woodall, J. Chem. Phys. **57**, 1547 (1972).
[34]T. S. Zwier, V. M. Bierbaum, G. B. Ellison, and S. R. Leone, J. Chem. Phys. **72**, 5426 (1980).
[35]J. O. Hirschfelder, C. F. Curtiss, and R. B. Bird, *Molecular Theory of Gases and Liquids* (Wiley, New York, 1964), p. 1126.
[36]R. C. Reid and T. K. Sherwood, *The Properties of Gases and Liquids* (McGraw-Hill, New York, 1966), p. 632.
[37]J. D. Lambert, *Vibrational and Rotational Relaxation in Gases* (Clarendon, Oxford, 1977), p. 109.
[38]T. A. Dillon and J. C. Stephenson, J. Chem. Phys. **58**, 2056 (1973).
[39]R. J. Cvetanovic, D. L. Singleton, and G. Paraskevopoulos, J. Phys. Chem. **83**, 50 (1979).

Downloaded 14 Jul 2006 to 129.63.184.195. Redistribution subject to AIP license or copyright, see http://jcp.aip.org/jcp/copyright.jsp